Bulletin de la Société belge de Géologie, T. 105 (1-2), 1996, pp. 41-59
Bulletin van de Belgische Vereniging voor Geologie. Ed. 1997

INTEGRATED GEOPHYSICAL/GEOLOGICAL MODELLING OF THE WESTERN BRABANT MASSIF AND STRUCTURAL IMPLICATIONS

Michel EVERAERTS [1], Christian POITEVIN [1], Walter DE VOS [2] & Marc STERPIN [2]

ABSTRACT. Integrated geophysical/geological modelling was carried out in an area of the western Brabant Massif in Belgium which is characterized by a strong negative Bouguer anomaly. Special attention was given to gravity modelling. A value of 2.10 g/cm³ was derived for the Bouguer reduction in order to minimize the effect of topography. The second vertical derivative of the gravity field was computed for different cell sizes in order to visualize strong contrast densities at different depths of investigation, and to deduce gravity lineaments.
A light granitic batholith is proposed to explain the gravity observations. Its shape and relationship to the surrounding rocks are discussed. A thorough structural analysis allows clarification of some elements of the geological history of the western Brabant Massif from early Ordovician times. The granite was probably intruded during early Silurian times, in deep crustal fracture zones inherited from Arenig rifting. The granite acted as a compact undeformed mass during the Acadian orogeny and a slightly younger strike-slip event. Later block faulting affected the western Brabant Massif and caused uplift of light granitic blocks.

KEYWORDS. Brabant Massif, Flanders (Belgium), granite, gravity, Bouguer anomaly, magnetic anomaly, geophysical modelling.

SAMENVATTING. In het westen van het Massief van Brabant werd een geïntegreerde geofysische en geologische modellering uitgevoerd van een gebied gekenmerkt door een sterke negatieve Bouguer anomalie. Vooral aan de gravimetrische analyse werd aandacht besteed. Voor de Bouguer reductie werd een dichtheid van 2.10 g/cm³ afgeleid, om het effect van de topografie te minimaliseren. De tweede vertikale afgeleide van het gravimetrisch veld werd berekend voor verschillende celafmetingen, om sterke contrasten in soortelijk gewicht op verschillende diepten te doen uitkomen, en gravimetrische lineamenten af te leiden.
De gravimetrische waarnemingen worden verklaard door de aanwezigheid van een lichte, granietische batholiet. Zijn vorm en verhouding tot het nevengesteente worden besproken. Een grondige structurele analyse laat toe enkele gebeurtenissen uit de geologische geschiedenis van het Massief van Brabant sinds het vroege Ordovicium op te helderen. De intrusie van de graniet vond vermoedelijk plaats in het vroege Siluur, langs diepe breukzones in de aardkorst die ontstaan waren gedurende een rifting episode in het Arenig. Het compact graniet bood weerstand tegen vervorming tijdens de Acadische orogenese en een jongere horizontaalverschuiving. Later werden lichtere granietische blokken selectief opgeheven bij de langzame vorming van het huidige schollengebied.

SLEUTELWOORDEN. Massief van Brabant, Vlaanderen (België), graniet, gravimetrie, Bouguer anomalie, magnetische anomalie, geofysische modellering.

RESUME. Une modélisation géophysique et géologique a été exécutée dans une partie du Massif du Brabant occidental caractérisée par une forte anomalie de Bouguer négative. Surtout l'analyse gravimétrique a fait l'objet d'une étude approfondie. Une valeur de 2.10 g/cm³ a été déduite pour la réduction de Bouguer, afin de minimaliser l'effet de la topographie. La seconde dérivée verticale du champ gravimétrique a été calculée pour des cellules de dimensions différentes pour visualiser des contrastes de densité à des profondeurs différentes, et de déduire des linéaments gravimétriques.

[1] Observatoire Royal de Belgique/Koninklijke Sterrenwacht van België, Avenue Circulaire 3 - B-1180 Bruxelles.
[2] Belgian Geological Survey, Jennerstraat 13, B-1000 Brussel.

Un batholithe granitique léger est proposé pour expliquer les observations gravimétriques. Sa forme et ses relations avec l'encaissant sont discutés. Une analyse structurale approfondie permet de clarifier certains éléments de l'histoire géologique du Massif du Brabant occidental depuis l'Ordovicien ancien. L'intrusion du granite a probablement eu lieu au début du Silurien, dans des zones de fracture crustale héritées du rift de l'Arenig. Le granite a agi comme une masse compacte non déformée pendant l'orogenèse acadienne et une phase décrochante subséquente. Plus tard, le Massif du Brabant a été compartimenté en blocs, soulevant les blocs granitiques plus légers.

MOTS-CLES. Massif du Brabant, Flandre (Belgique), granite, gravimétrie, anomalie de Bouguer, anomalie magnétique, modélisation géophysique.

1. INTRODUCTION

The aim of this paper is to publish the most important results and conclusions of a geophysical modelling study carried out in the western part of the Brabant Massif (Everaerts, 1993). This area is characterized by the elongated gravity low of Flanders, and a complex pattern of magnetic anomalies. The Lower Palaeozoic rocks are concealed under Cretaceous and Tertiary cover, and its geology is known from scattered boreholes, about 160 of which have yielded core samples.

It has been recognized before that the negative Bouguer anomaly of Flanders can best be explained by a concealed granite (de Magnée, 1949; De Meyer, 1983, 1984; André, 1991; Chacksfield *et al.*,1993; De Vos *et al.*, 1993c; Hennebert, 1994). Although there is enough evidence from boreholes for a volcanic arc running south of the antiformal axis of the Brabant Massif, granitic rocks have never been reached by drilling.

The present study integrates geological, gravity and magnetic data to determine the shape and extension of the granite, while also modelling the typical features of the neighbouring geological units. This approach was made possible by the renewed interest in the Anglo-Brabant Massif, which stimulated new data acquisition and reprocessing of existing data. Two international symposia documented this recent research (Verniers *et al.*, 1991; Pharaoh *et al.*, 1993). The results of preliminary modelling were published by Chacksfield *et al.* (1993). The geological framework used for the present modelling is taken from a new geological subcrop map (De Vos *et al.*, 1993a).

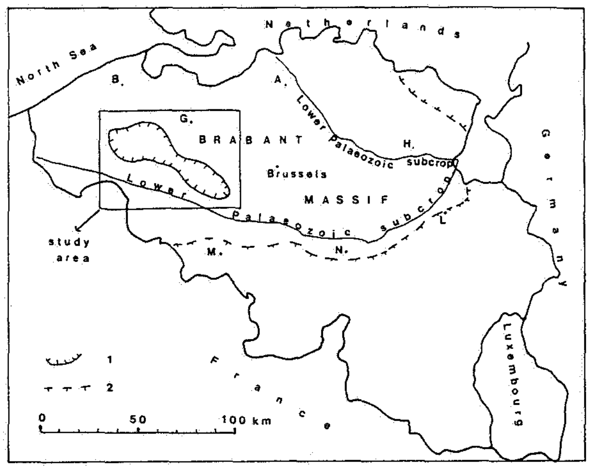

Figure 1. Location map of the study area in Belgium. 1. Gravity low of Flanders. 2. Gravity gradient bordering Brabant Massif at depth. Cities: A Antwerpen, B Brugge, G Gent, H Hasselt, L Liège, M Mons, N Namur.

New high precision gravity surveys with a point density of 1 station per km² were carried out recently by the Observatoire Royal de Belgique/Koninklijke Sterrenwacht van België (ORB-KSB) in the area of the gravity low of Flanders, and the 1963 aeromagnetic map of Belgium was digitised at the Belgian Geological Survey, providing the opportunity for detailed modelling.
The modelled area (figure 1) is limited by the following Belgian Lambert coordinates: X from 58.0175 to 130.0175 km, and Y from 148.175 to 198.175 km. This rectangle of 3 600 km² encompasses 45 topographical map sheets at a scale of 1/10 000.

2. GEOPHYSICAL DATA

2.1. THE MAGNETIC DATA

The Belgian aeromagnetic survey was flown in 1963, the flying height in this part of the country being 2000 feet above sea level. The orientation of the flight lines was N30°E with a spacing of 2.5 km. Perpendicular tie-lines were flown 10 km apart. Contour maps of the magnetic total field were produced at a scale of 1/100 000 from the analog recording, and a generalized map at 1/300 000 was produced (Belgian Geological Survey, 1964). During a Belgian-British research project, the contour maps were digitised and validated, and image-based display techniques were applied to the digital data set, highlighting magnetic lineaments and deep structural trends for the whole of Belgium (De Vos *et al.*, 1993b; Chacksfield *et al.*, 1993).

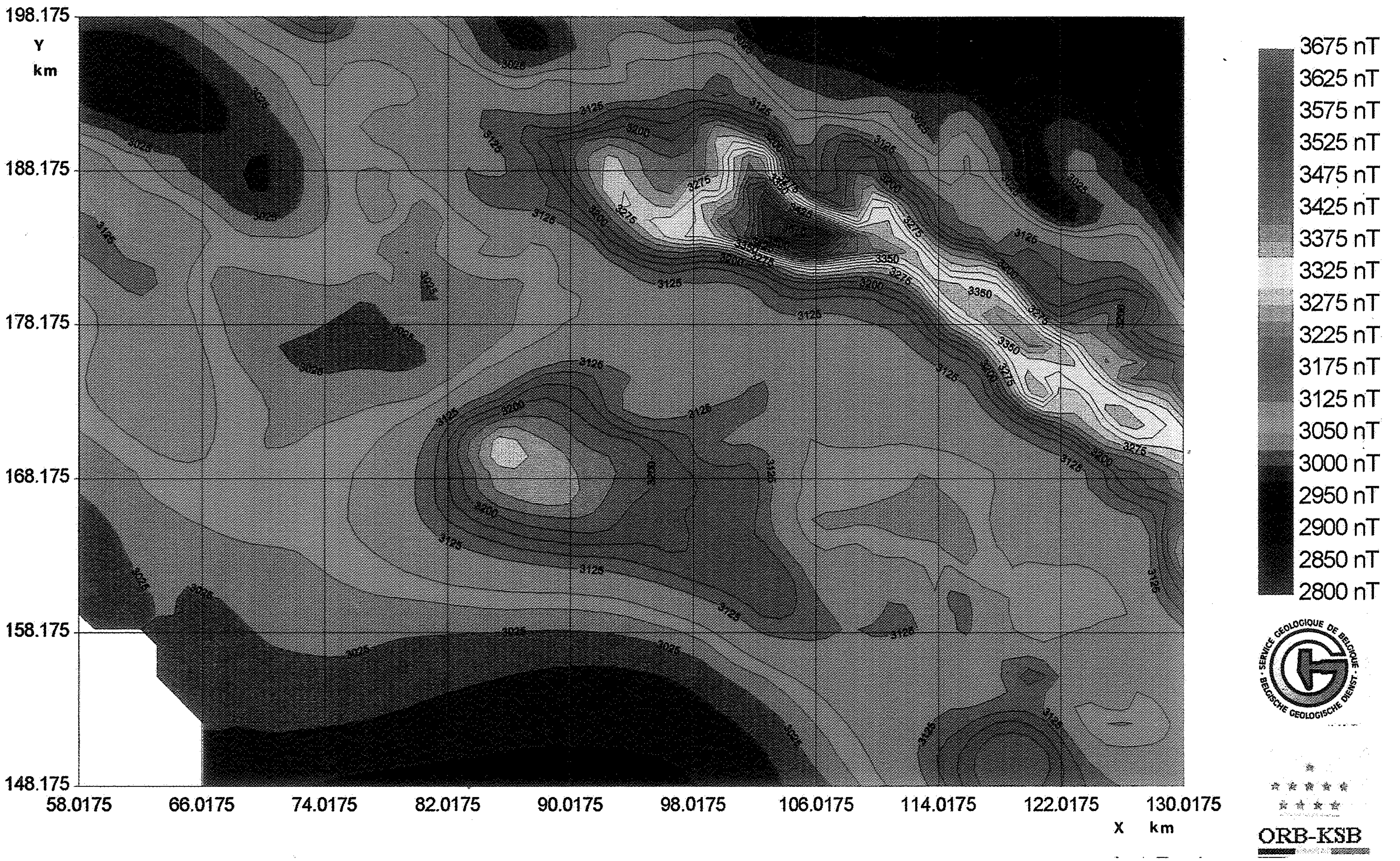

Figure 2. Aeromagnetic total field map of the study area (1963 survey). Relative magnetic intensity in nanoTesla (nT). Coordinates in km in Belgian Lambert system, with indication of topographic map sheets.

This existing digital data set was used for the present study. Figure 2 shows a colour contour map of the total magnetic field in the modelled area. An inclination of 66.17° and a declination of -5.5° (to the west) together with an average magnetic field of 46 500 nT (nanoTesla) were used.

2.2. THE GRAVITY DATA

Data from four different sources were merged in the gravity compilation:
(i) the igm4748 survey of Belgium comprising 373 stations (Jones, 1949);
(ii) the igm6272 survey in northwestern Belgium with an average point density of 2.5 observations per km^2 (unpublished);
(iii) the Ardooie survey carried out by the ORB-KSB in 1986 with an average spacing of 1 station per km^2 (Poitevin, 1987, 1989);
(iv) the Oudenaarde survey carried out by the ORB-KSB in 1991-1992 with the same spacing as in Ardooie (Poitevin, 1992).
Hence, gravity data were available for most of the study area with a minimum observation density of one station per square kilometer. The data set was validated by the ORB-KSB.

For the Bouguer terrain correction, the Nettleton (1939) method was applied to estimate the surface density, with values varying from 2.00 to 2.70 g/cm^3. This was done to select the appropriate mass density for the superficial rocks above sea level, i.e. Tertiary sand and clay, in order to minimize the effect of topography at the Bouguer reduction. The best result was obtained with a reduction density of 2.10 g/cm^3 for all the data.
The data were interpolated on a 1 km^2 regular grid and a colour contour map of the Bouguer gravity anomaly was produced (figure 3). Two gravity minima can be observed, an eastern one centered around Deftinge, elongated NW-SE following the general trend of the gravity low, and a western one, centered around Oostrozebeke, showing an elongation transverse to the main trend.

3. GEOLOGY AND PETROPHYSICAL DATA

Figure 4 presents an extract from the geological Pre-Permian subcrop map of the Brabant Massif (De Vos *et al.*, 1993a). The Bouguer anomaly contour lines are overlain on the geology.
The oldest rocks in the study area (green in fig.4) belong to the Tubize group, consisting of phyllite, siltstone and fine to coarse sandstone or quartzite with varying feldspar content. They are characterized by their green colour, due to epimetamorphic chlorite, and frequent magnetite-bearing horizons. The age is early Cambrian (Verniers & De Vos, 1995). The magnetic susceptibility of the Tubize group rocks is rather high, though variable, and could explain most of the observed magnetic anomaly (De Vos *et al.*, 1993c).
The Oisquercq group (purple in fig.4) contains greenish, purplish or grey phyllites and siltstones, without magnetite and poorly stratified. Its age is late early to early middle Cambrian.
The upper Cambrian (dark blue in fig.4) is represented in the central and eastern part by the Mousty formation, composed of dark grey to black shale. In the north-east of the area, the upper Cambrian is represented by the grey Jodoigne quartzite.
The Tremadoc (lower Ordovician, pale brown in fig.4) contains grey turbiditic sequences with a typical layered lithology, lighter sandstone and siltstone being dominant over darker claystone. Younger Ordovician rocks (dark red in fig.4) are generally darker and more fine-grained. The Silurian (pale red in fig.4) consists of dark grey mudstones and mostly fine-grained turbidites.
The sedimentary rocks from the Oisquercq group up to the Silurian are difficult to differentiate petrophysically (De Vos *et al.*, 1993c). They show only a weak background magnetic susceptibility, and their densities show a narrow range of observed measurements. The density figures used for the modelling are the best estimates to fit the gravity curves.

To the southwest of the area, Carboniferous calcareous rocks (light blue in fig.4) are found, sometimes overlying sandy upper Devonian rocks (dark brown on the map). These Upper Palaeozoic rocks lie unconformably on top of the Brabant Massif basement. In the study area, however, a faulted contact could occur locally between the Lower and Upper Palaeozoic rocks.

Many magmatic rocks are found (bright red with vv ornament in fig.4), either as interstratified volcanic rocks in the upper Ordovician (small v), or as relatively small intrusive bodies (large V) within the same arc, extending from northwest to southeast through the study area. The known magmatic rocks have a range of mass densities similar to the sedimentary rocks, and cannot account for the huge negative Bouguer anomaly, which is parallel to the volcanic arc, but slightly offset to the north with respect to the main volcanic occurrences in the eastern and central part (figure 4).

The general structure of the study area, deduced from the subcrop map, is characterized by west-north-west striking antiforms and synforms.

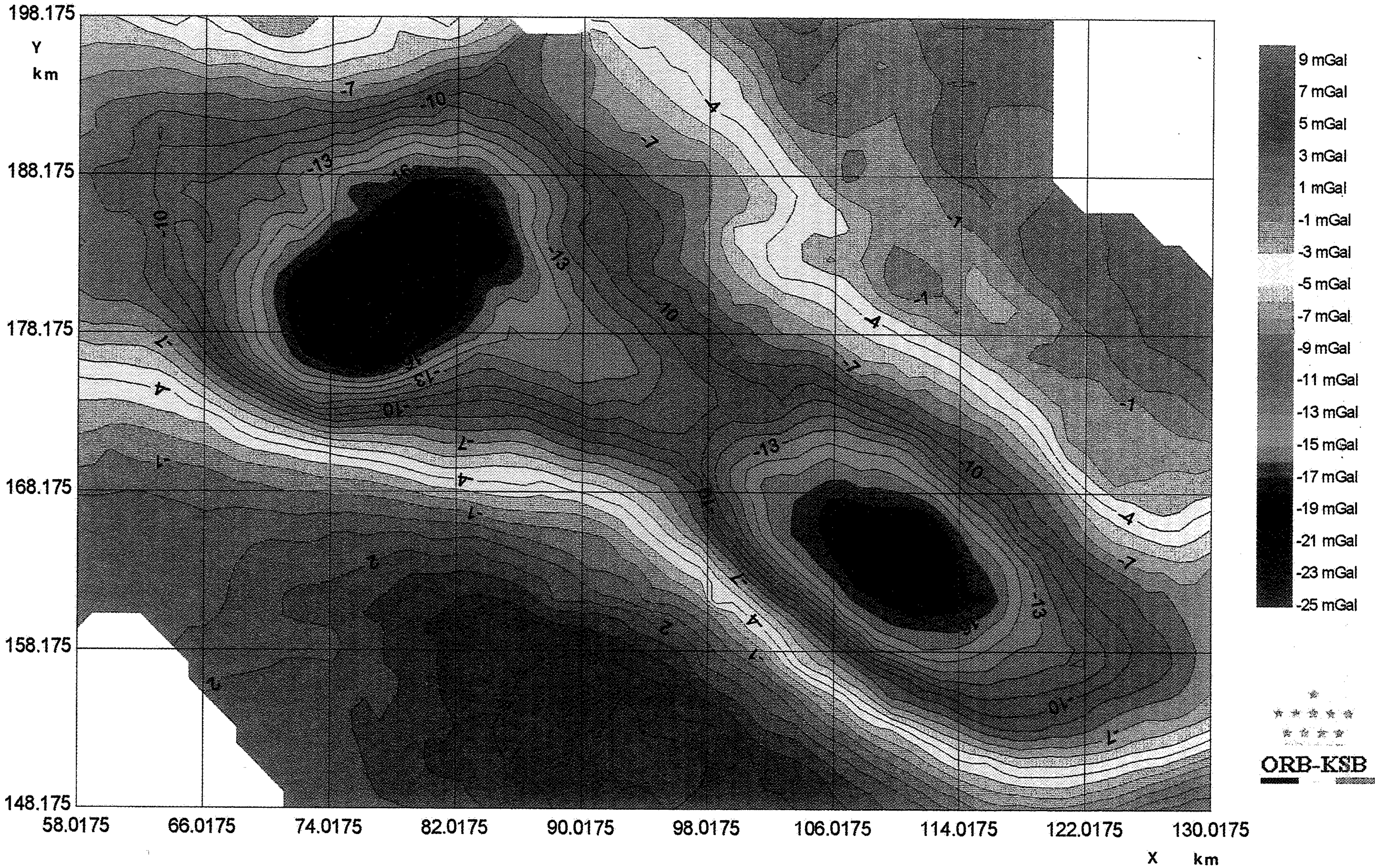

Figure 3. Bouguer anomaly map in the study area. Relative gravity field in milliGal. Coordinates in km in Belgian Lambert system, with indication of topographic map sheets.

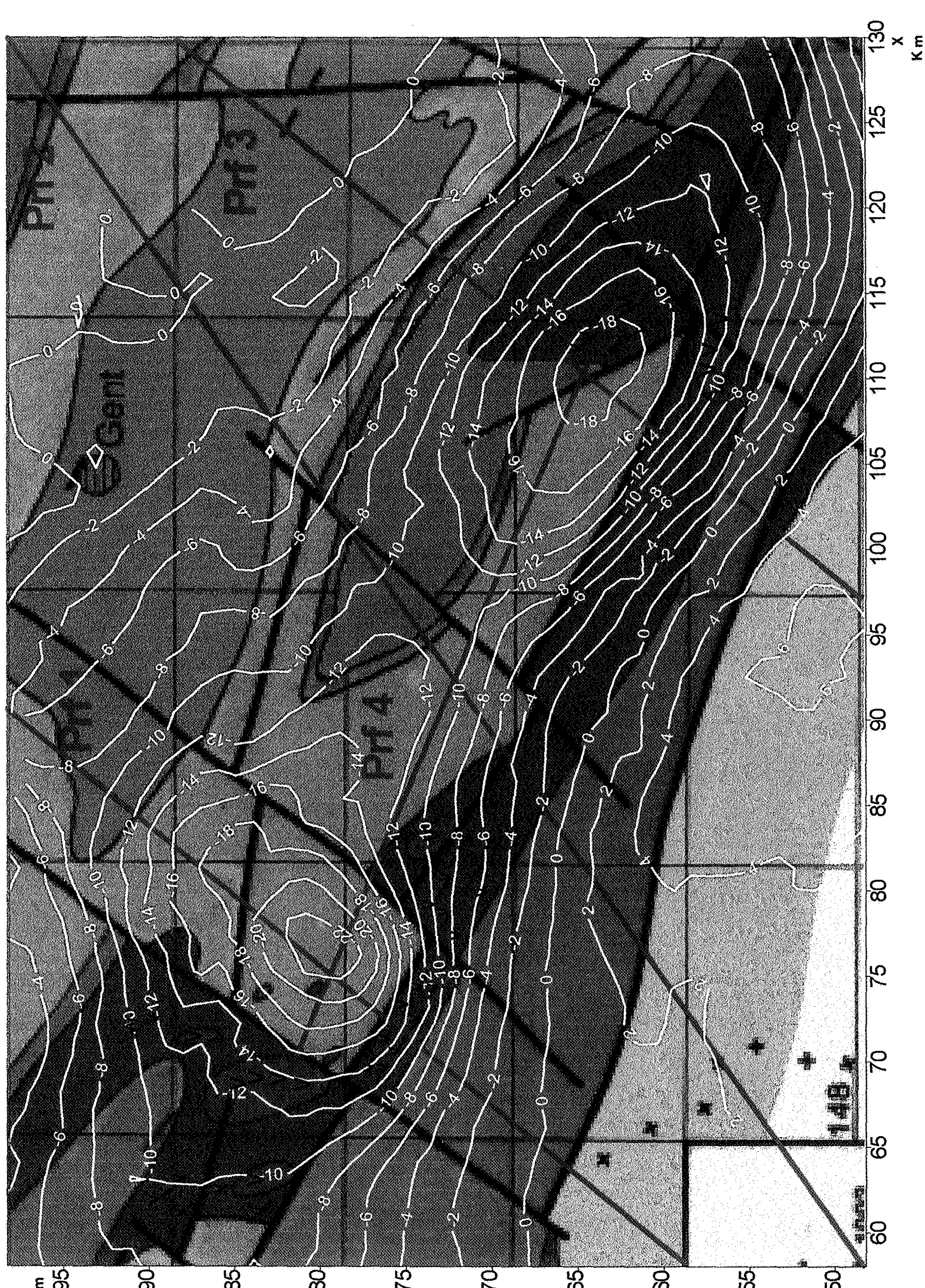

Figure 4. Geological subcrop map of Palaeozoic basement in study area, according to De Vos *et al.* (1993), with gravity overlay and location of the four modelling profiles Prf1 to Prf4. Coordinates in km in Belgian Lambert system, with indication of topographic map sheets. Green: Tubize group. Purple: Oisquercq group. Dark blue: upper Cambrian. Pale brown: Tremadoc. Dark red: middle and upper Ordovician. Ornament vv: magmatic rocks; small v: interstratified, large V: small intrusive bodies. Pale red: Silurian. Dark brown: middle to upper Devonian. Light blue: Carboniferous.

In the north there is an antiform of Tubize group rocks, which are always found in subvertical position. South of this antiform, there is a synform plunging to the southeast, with upper Cambrian to upper Ordovician sediments in its core, and another westward plunging synform, with younger rocks of upper Ordovician to Silurian age. In between, the synform is interrupted by a transverse antiform, probably a horst, of Oisquercq group rocks. The Oisquercq group is rather continuous in the subcrop in the study area, and always separates the Tubize group from upper Cambrian and younger rocks. An unconformity between the Oisquercq group and all younger sedimentary strata is probable. It is worth mentioning that the Oisquercq group has a much larger extension in this subcropping part of the Brabant Massif, as deduced from borehole data, than in the outcrop area to the south-east of the present study area.
A second unconformity, between the Tremadoc and the upper Ordovician, is probable: no rocks of Arenig age have been identified with certainty in the Brabant Massif, whereas Llanvirn age rocks have yet to be confirmed.
A second antiform, probably a horst structure, is present in the south of the study area. Here, the Oisquercq group comes closer to the surface, whereas the strong magnetic anomaly in this area is an indication of the underlying Tubize group. South of this horst, upper Ordovician strata dip gently to the southwest, concordantly overlain by Silurian rocks.
Longitudinal and transverse faults occur, in a block faulting pattern. The faults were mostly drawn from geophysical evidence, either magnetic or gravimetric or both.

The subcrop map shows only the top of the lower Palaeozoic basement. One of the objectives of the present modelling is to provide deep geological cross sections through the Brabant Massif, constrained by the potential field data (gravity and magnetic).
The granite and the Tubize group determine to a large degree the pattern of respectively the gravity and the magnetic curves. Hence, they will be the most prominent lithological features of these deep profiles.

4. GRAVITY PROCESSING BY THE SECOND VERTICAL DERIVATIVE TECHNIQUE (SVD)

Batholith-like granitic bodies are commonly associated with negative gravity anomalies, due to the low density of the batholith compared to the density of the surrounding rocks. The major aim of our gravity interpretation is to determine the batholith configuration from these anomalies.
Mapping the Second Vertical Derivative (SVD) of the gravity field is very helpful to achieve this goal. It has the advantage that gravity data transformed to the vertical gradient, can be effectively processed in three dimensions in order to delineate density discontinuities or contrasts (Marson & Klingele, 1993). It allows to obtain images of the intrusive body at different depths and to define fault-like lineaments.

4.1. SVD COMPUTATION

Several algorithms are available to compute the SVD: Henderson & Zietz (1949), Peters (1949), Elkins (1951), Rosenbach (1953), Baranov (1953). They all have advantages and disadvantages. Most of them are designed to be used with circular templates, which is a major drawback. As our data form a regular grid, we have written a programme based on the Haalck method (Morelli, 1968) which is much more convenient for computer calculation.
We briefly present here the formulae which were used.
Poisson's formula can be written as:

$$\frac{\partial^2 U}{\partial x^2}+\frac{\partial^2 U}{\partial y^2}+\frac{\partial^2 U}{\partial z^2}=4\pi k\rho$$

where U is the gravitational potential and ρ is the mass density at the considered point, with k a proportionality constant.
At first approximation we can consider that $\rho \cong \rho(z)$. This means that we neglect the atmosphere and consider that all the superficial mass has been condensed on an ellipsoid or an equivalent reference surface.
In this case:

$$\frac{\partial}{\partial z}\left[\frac{\partial^2 U}{\partial x^2}+\frac{\partial^2 U}{\partial y^2}+\frac{\partial^2 U}{\partial z^2}\right]=0$$

which can be rewritten as:

$$\frac{\partial^2}{\partial x^2}\left[\frac{\partial U}{\partial z}\right]+\frac{\partial^2}{\partial y^2}\left[\frac{\partial U}{\partial z}\right]+\frac{\partial^2}{\partial z^2}\left[\frac{\partial U}{\partial z}\right]=0$$

We know that: $\frac{\partial U}{\partial z}=g$

then:

$$\frac{\partial^2 g}{\partial x^2}+\frac{\partial^2 g}{\partial y^2}+\frac{\partial^2 g}{\partial z^2}=0$$

which becomes:

$$\frac{\partial^2 g}{\partial z^2}=-\left[\frac{\partial^2 g}{\partial x^2}+\frac{\partial^2 g}{\partial y^2}\right]$$

The SVD can then be directly computed for any station, based on the surrounding values.

The Haalck method defines the form of a matrix operator which runs in the X and Y directions. This operator acts as a high-pass filter in two dimensions. It can be described as follows:
Consider a large square subdivided into four smaller squares, the smaller squares defining the gridding cell size, with side s. The Bouguer anomaly values were interpolated by gridding at the corners of the small squares, numbered from 1 to 8 around the periphery of the large square, and 9 in the center of the figure. The horizontal gradient at the centers of the small squares, P_1, P_2, P_3, P_4, can be calculated using the Bouguer anomaly values at the corners, using the formulae:

$$\left(\frac{\partial g}{\partial x}\right)_{P_1} = \frac{1}{2}\left(\frac{g_1-g_8}{s}+\frac{g_2-g_9}{s}\right) \qquad \left(\frac{\partial g}{\partial y}\right)_{P_1} = \frac{1}{2}\left(\frac{g_2-g_1}{s}+\frac{g_9-g_8}{s}\right)$$

$$\left(\frac{\partial g}{\partial x}\right)_{P_2} = \frac{1}{2}\left(\frac{g_2-g_9}{s}+\frac{g_3-g_4}{s}\right) \qquad \left(\frac{\partial g}{\partial y}\right)_{P_2} = \frac{1}{2}\left(\frac{g_3-g_2}{s}+\frac{g_4-g_9}{s}\right)$$

$$\left(\frac{\partial g}{\partial x}\right)_{P_3} = \frac{1}{2}\left(\frac{g_9-g_6}{s}+\frac{g_4-g_5}{s}\right) \qquad \left(\frac{\partial g}{\partial y}\right)_{P_3} = \frac{1}{2}\left(\frac{g_4-g_9}{s}+\frac{g_5-g_6}{s}\right)$$

$$\left(\frac{\partial g}{\partial x}\right)_{P_4} = \frac{1}{2}\left(\frac{g_8-g_7}{s}+\frac{g_9-g_6}{s}\right) \qquad \left(\frac{\partial g}{\partial y}\right)_{P_4} = \frac{1}{2}\left(\frac{g_9-g_8}{s}+\frac{g_6-g_7}{s}\right)$$

In the same way we can compute the average horizontal second derivative at the center of the figure (point 9) using the formulae:

$$\left(\frac{\partial^2 g}{\partial x^2}\right)_9 = \frac{1}{2}\left[\frac{\left(\frac{\partial g}{\partial x}\right)_{P_1}-\left(\frac{\partial g}{\partial x}\right)_{P_4}}{s}+\frac{\left(\frac{\partial g}{\partial x}\right)_{P_2}-\left(\frac{\partial g}{\partial x}\right)_{P_3}}{s}\right]$$

$$\left(\frac{\partial^2 g}{\partial y^2}\right)_9 = \frac{1}{2}\left[\frac{\left(\frac{\partial g}{\partial y}\right)_{P_2}-\left(\frac{\partial g}{\partial y}\right)_{P_1}}{s}+\frac{\left(\frac{\partial g}{\partial y}\right)_{P_3}-\left(\frac{\partial g}{\partial y}\right)_{P_4}}{s}\right]$$

The sum of the two equations, with a negative sign, gives the SVD:

$$\left(\frac{\partial^2 g}{\partial z^2}\right)_9 = \frac{1}{2s^2}[4g_9-(g_1+g_3+g_5+g_7)]$$

The second vertical derivative is more interesting than the first derivative due to its high discriminating power. The physical significance of the SVD is to represent the trend of the spatial variation of the gravity field calculated along the vertical axis. It allows examination of the curvature irregularities of a residual surface of the original field, after subtraction of the long period waves. The SVD thus enables us to isolate the more rugged and shallower anomalies by removing trends which are more regional in comparison.

It follows from the method that the zero values of the SVD indicate the maximum of the original field gradient, this is the transition between concave and convex areas of the potential field surface. Thus the zero contour lines of the SVD point to steep-sloping contacts or even vertical borders between rocks of different mass density. In this way deep, steep faults juxtaposing rocks with strong density contrasts can be located.

4.2. APPLICATION TO THE STUDY AREA

The SVD method was tested in the study area. Modifying the cell size of the calculation corresponds to modifying the depth of investigation. A cell with a small size visualizes shallow density contrasts, whereas a larger cell size shows deeper density contrasts.
Indeed, the zero contour line of the SVD corresponds to the curvature change from convex to concave of the Bouguer anomaly or vice-versa. For a specific cell size, e.g. 5 km (fig.5), a map of this zero contour line helps to determine the horizontal extension of the light intrusive body at a certain depth. By gradually decreasing the cell size, horizontal sections through the body at ever shallower depth seem to appear.
The picture becomes blurred however for the shallow sections (smaller cell size), because the granite becomes smaller and finally disappears. Close to the surface, too many different lithologies are involved, and also some noise appears close to the limit of the resolution of the SVD method, determined by the observation point density of 1 per km^2.
However, the deeper sections (larger cell size) allow to deduce the shape and size of the batholith in three dimensions.
Figure 5 shows the zero contour line of the SVD for cell sizes between 5 km and 2 km.
An empirical formula gives the relationship between the size of the cell (s) and the depth (D) of the horizontal section:

$$D \le \frac{\frac{x}{2}}{(4^{1/3}-1)}$$

with $\quad 2s \le x \le 2\sqrt{2}s \quad$ or $\quad 1.3s \le D \le 1.8s$

As an example, a cell size of 5 km (fig.5) gives a picture of the density contrasts at a depth of 6.5 to 9 km. A cell size of 3 km visualizes the density contrasts at a depth of 3.9 to 5.4 km. From the different zero contour lines of the SVD, it appears that the southern limit of the granite is always at the same geographical location regardless of cell size, so that this southern border should be roughly vertical.

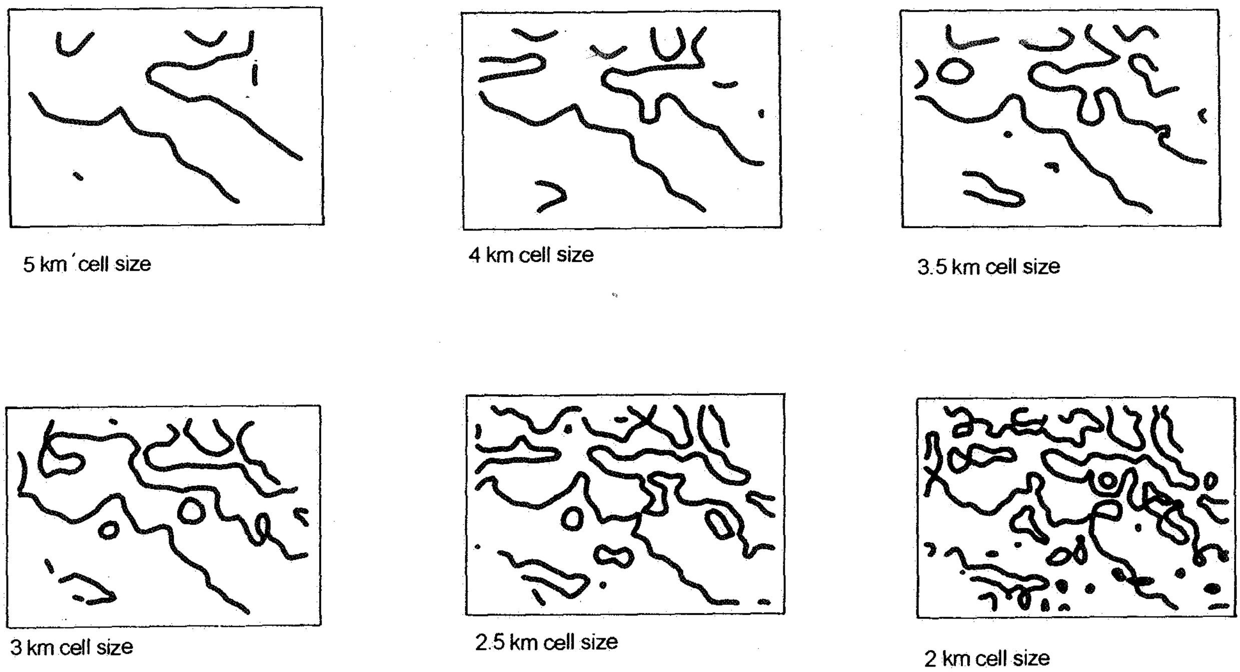

Figure 5. Maps of study area at reduced scale with position of zero contour line of the second vertical derivative (SVD) of the gravity field for different cell sizes (explanation see text).

Figure 6 shows a synthetic map of the lineaments deduced from the SVD of the gravity field. Several faults, especially transverse ones with orientation NE-SW, already drawn on the geological map (De Vos *et al.*, 1993a), are confirmed or slightly modified. The southern limit of the granite is not rectilinear (fig.6). It appears as line segments roughly directed west-north-west. A tentative geological interpretation is given below.

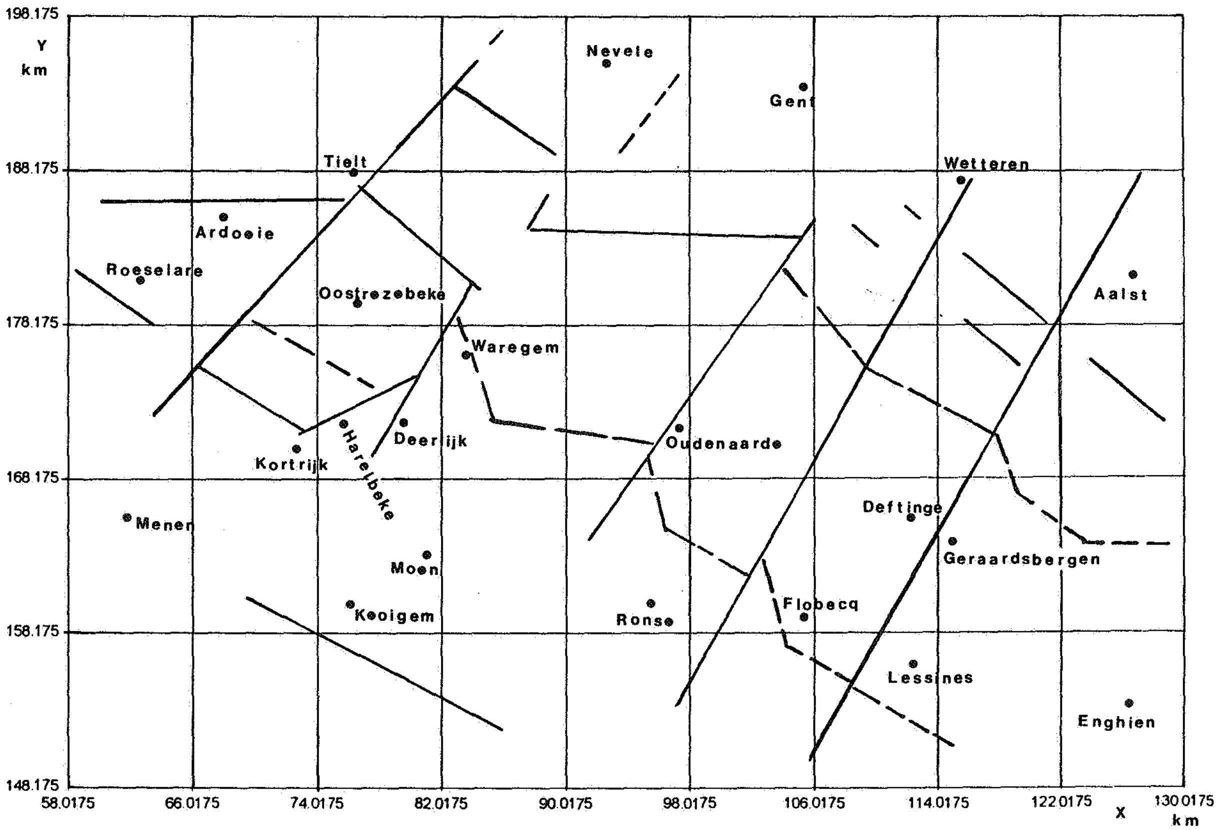

Figure 6. Gravity lineaments indicating vertical faults or lithological discontinuities in the study area, as deduced from the second vertical derivative of the gravity field. Localities cited in text or profiles are added.

Apart from the shape of the granite, some lineaments in the northeast of the area coincide with the core of the Tubize antiform, where alternating phyllitic and quartzitic rocks are probably responsible for the density contrast.

5. INTEGRATED MODELLING IN VERTICAL PROFILES

5.1. METHOD

In order to obtain a three-dimensional picture of the deep structure of the study area, geophysical modelling was realized using the GravMag program developed at the British Geological Survey (Pedley, 1991). GravMag is a highly interactive program for simultaneous 2.5D modelling of gravity and magnetic data.

The software enables the operator to construct and edit realistic geological models, by defining polygons of different lithology in a vertical plane, each with a distinct mass density and magnetic susceptibility. The profile has a finite width, typically between 1 and 4 km, and thus represents a vertical slice through the crust (hence the qualification "2.5D" for 2.5 dimensional). The theory for the gravity calculation is taken from Rasmussen & Pederson (1979), and for the magnetic calculation from Shuey & Pasquale (1973).

A series of profiles were modelled across the gravity low of Flanders (Everaerts, 1993). A corresponding geological cross section has been presented for two of

	Density (g/cm^3)	Magnetic susceptibility (S.I. units)	Figure 7, profile 1	Figure 8, profile 2	Figure 9, profile 3	Figure 10, profile 4	Figure 10, half strike (km)
Background	2.700	0.000	fig. 7	fig. 8	fig. 9	fig. 10	
Granite	2.630	0.000	red	red	red	red	10
Granite	2.630	0.000				brown	5
Granite	2.630	0.000				bluish	9
Tubize group	2.720	0.020	polygon 1 polygon 3		polygon 7 polygon 9	polygon 10	10
Tubize group	2.690	0.030			polygon 12		
Tubize group	2.720	0.040		polygon 4 polygon 6			
Tubize group	2.750	0.040		polygon 11			
Tubize group	2.720	0.050	polygon 2			polygon 2	10
Tubize group	2.720	0.100		polygon 5	polygon 8	polygon 5 polygon 8	10
Tubize or Oisquercq	2.720	0.004				polygon 13	10
Oisquercq group	2.700	0.004	purple	purple	purple	purple	10
Upper Cambrian to Silurian sediments	2.750	0.000	orange	yellow, orange	orange	orange	10
Geraardsbergen diorite	2.750	0.034				black polygon 1	0.5
Ardooie porphyritic rock	2.680	0.000				grey polygon 3	5
Devonian to Carboniferous	2.700	0.000	blue	blue	blue		

Table 1. Petrophysical properties: mass density and magnetic susceptibility used to construct the different polygonal bodies in the modelled geological sections.

them (De Vos, 1993). This paper discusses the modelling of three selected profiles transverse to the main structure of the Brabant Massif, and one parallel to the longitudinal axis. Their location is indicated on figure 4. Profile 1 (figure 7) is a section across the western gravity minimum of Oostrozebeke, profile 2 (figure 8) across the central part of the gravity low near Oudenaarde, and profile 3 (figure 9) across the eastern gravity minimum of Deftinge.
Profile 4 (figure 10) represents a profile running through the whole granite, allowing an interpretation along its longitudinal axis. In figures 7 to 10, some localities lying close to the profiles are indicated; they are mapped on figure 6.

The geological control for all the profiles was based on the subcrop map of the Brabant Massif (De Vos *et al.*, 1993a) and on borehole information. Small deviations from the subcrop map were allowed, where borehole information is scarce and limits between geological units on the map had been drawn on the basis of geophysical information.

The geophysical effect of the unfolded Cretaceous and Cenozoic cover rocks, with a thickness varying from 50 to 150 m, is considered negligible. As the models were drawn without vertical exaggeration, the cover rocks are too thin to be represented.

Table 1 presents the different petrophysical properties of the polygons used to construct profiles 1 to 4, with their geological meaning.
The petrophysical properties assigned to the different lithological polygons were kept as close as possible to the results of density measurements performed at the Fina Research laboratory, and the corresponding magnetic susceptibility values determined at the Centre de Physique du Globe (De Vos *et al.*, 1993c). However, as these figures showed a large variance for each geological type, the average figures were modified by trial and error, until a satisfactory fit was achieved between the calculated curves and the observed ones, for both gravity and magnetism (upper charts of figures 7 to 10), while keeping the cross sections geologically realistic. The Tubize group especially was found to display a large variation in rock properties, especially magnetic susceptibility.
For the purpose of the GravMag computing, the petrophysical properties are supposed to extend in the direction perpendicular to the profile to a certain distance, called half strike; it was set at a standard 30 km for profiles 1 to 3 which run across the structures. For profile 4 (figure 10) which runs parallel to the structure, the different geological bodies have a narrower extension perpendicularly to the profile; accordingly a different half strike was applied for each polygon (table 1). All rocks beyond the half strike are supposed to have background properties in the modelling.

5.2. THE GRANITE

In profiles 1 to 3, the granite is indicated in red. In profile 4, it is subdivided into three segments having a different half strike: 10 km in the western part (red in figure 10), 5 km in the central part (brown) and 9 km in the eastern part (bluish purple).
From the trial modelling it is apparent that the strong negative Bouguer anomaly requires a density contrast between the intrusive body and the neighbouring rocks in the order of 0.07 g/cm^3 or more.
A mass density of 2.63 g/cm^3 was assigned to all segments of the granite. This figure was also used by Chacksfield *et al.* (1993) and is based on similar modelling in the English Lake District (Lee, 1989) and in southern England (Busby *et al.*, 1993), where granites are intruded in a similar lower Palaeozoic setting in the prolongation of the Brabant structure. A rock density higher than 2.63 g/cm^3 would require the batholith to be larger or shallower in order to cause a similar Bouguer anomaly. However, it cannot be larger because of the SVD constraint; and if it were shallower, the gravity anomaly would have a smaller wavelength response at the surface. Conversely, a density lower than 2.63 g/cm^3 would mean a quartz-rich granite at greater depth; again, this would result in a different shape of the observed gravity curve.

The width of the granite was modelled using the zero contour line of the second vertical derivative of the gravity field (see above). This is a first constraint on the shape of the concealed granite. Near-vertical faults are thought to run along most of its periphery. The northern and southern granite boundaries are assumed to be near-vertical faults. The granite most probably corresponds to a horst structure.

The roof of the granite appears at different depths. Profile 4 (figure 10) shows that the granite consists of three segments not only on the basis of its width, but also of its depth. At both Oostrozebeke in the west and Deftinge in the east, it reaches a depth below the surface of 1 to 2 km, giving rise to both gravity minima. In the central segment around Oudenaarde, the roof is at a depth of 4 to 6 km, causing the gravity low to be weaker. Transversal profiles 1 to 3 further illustrate this picture. The longitudinal variation can be explained by a breakup of the granite in a horst-graben pattern by block faulting. It is also possible that it was not intruded to the same crustal level in the central part.

In the western part of the longitudinal profile (figure 10), the model does not fit the observed gravity curve in an optimal way; at this place the intrusion could be locally shallower than elsewhere, because of the sharp gravity curve. However the observed gravity curve in the transverse profile (figure 7) is less sharp. A more

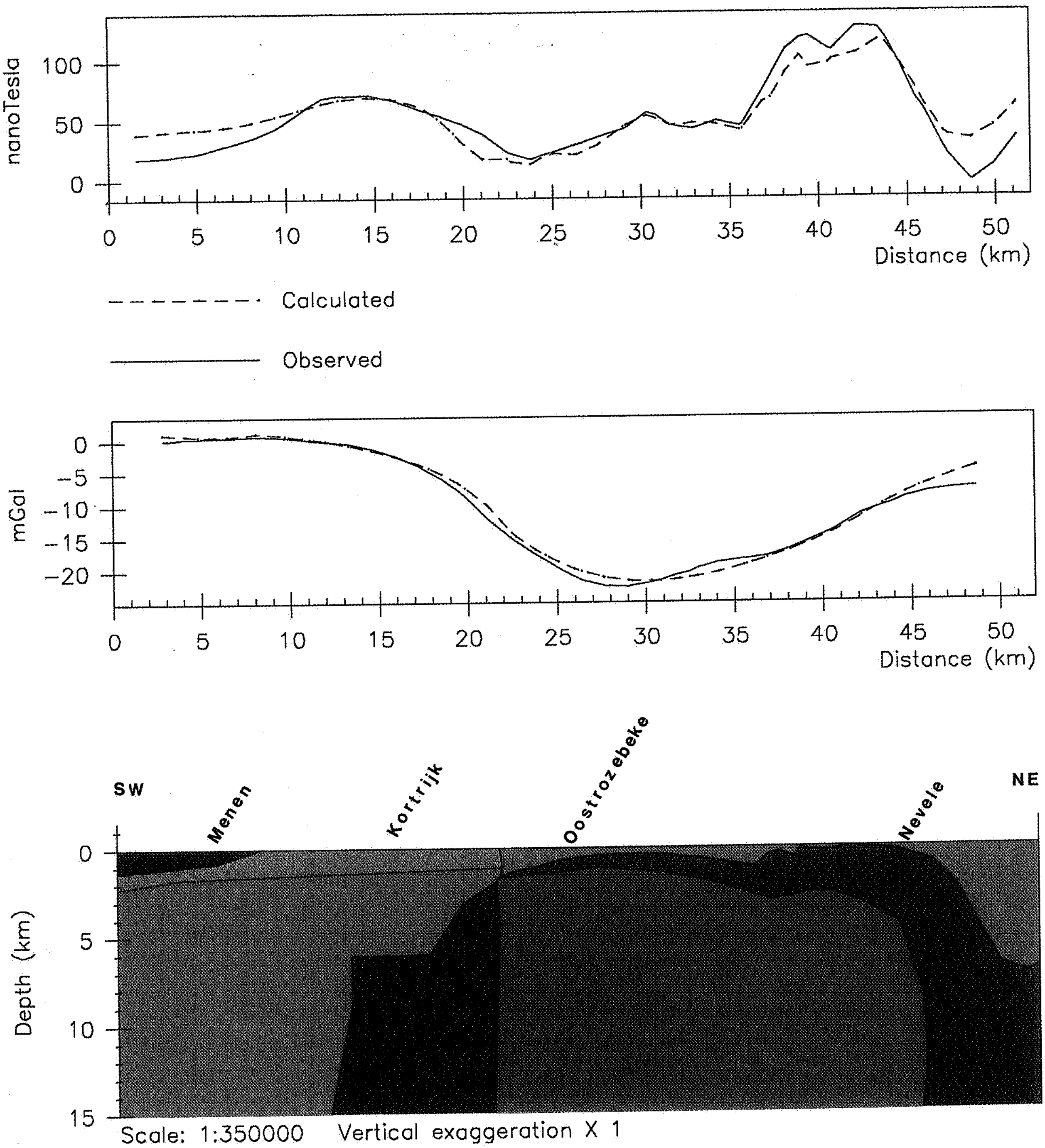

Figure 7. Modelled geological section along profile 1 (location see figure 4), across western gravity minimum. Upper figure: magnetic curve; middle figure: gravity curve; lower figure: geological model. Polygon numbers and their petrophysical properties assumed in the model are presented in table 1. Red: granite. Green: Tubize group. Purple: Oisquercq group. Orange: Ordovician and Silurian sediments. Blue: Devonian and Carboniferous.

coherent picture with a better resolution would only be obtained if additional gravity data were measured at a much greater observation density than the present 1 point per km^2.

The precise shape of the granite and the depth of its roof should be viewed with caution. The resolution of the model is limited by the gravity data density. Moreover, some inaccuracy is inherent in each modelling, and a balance has to be struck between three independent variables: the mass density, the total volume and the depth. It should be kept in mind that the granitic body has not been reached by drilling.

5.3. THE TUBIZE GROUP

After establishing the shape of the granite in the profiles, the next geological unit with a typical geophysical signature is the magnetic Tubize group.

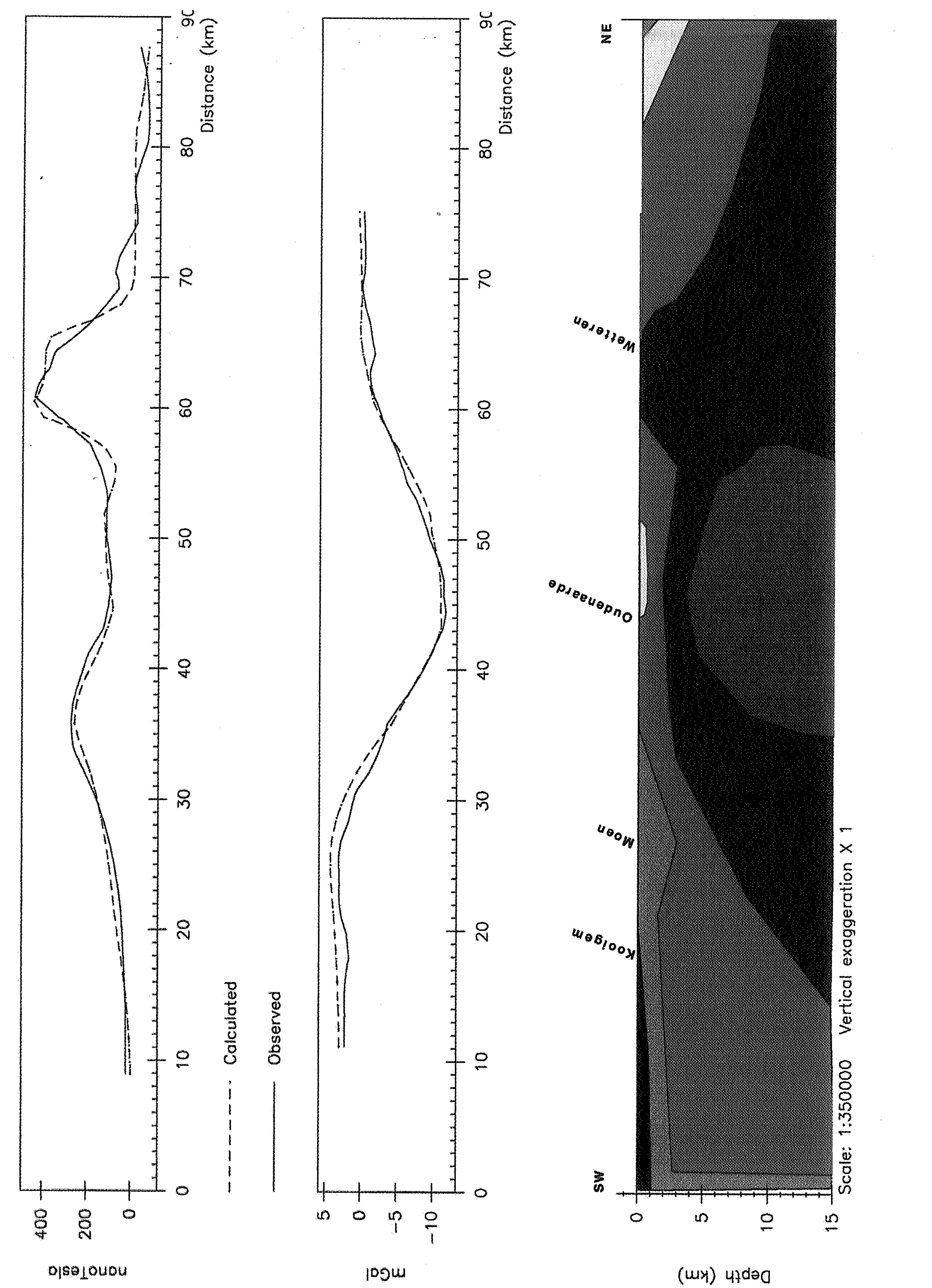

Figure 8. Modelled geological section along profile 2 (location see figure 4), across central gravity low. Upper figure: magnetic curve; middle figure: gravity curve; lower figure: geological model. Polygon numbers and their petrophysical properties assumed in the model are presented in table 1. Red: granite. Green: Tubize group. Purple: Oisquercq group. Yellow: upper Cambrian and Tremadoc sediments. Orange: Ordovician and Silurian sediments. Blue: Devonian and Carboniferous.

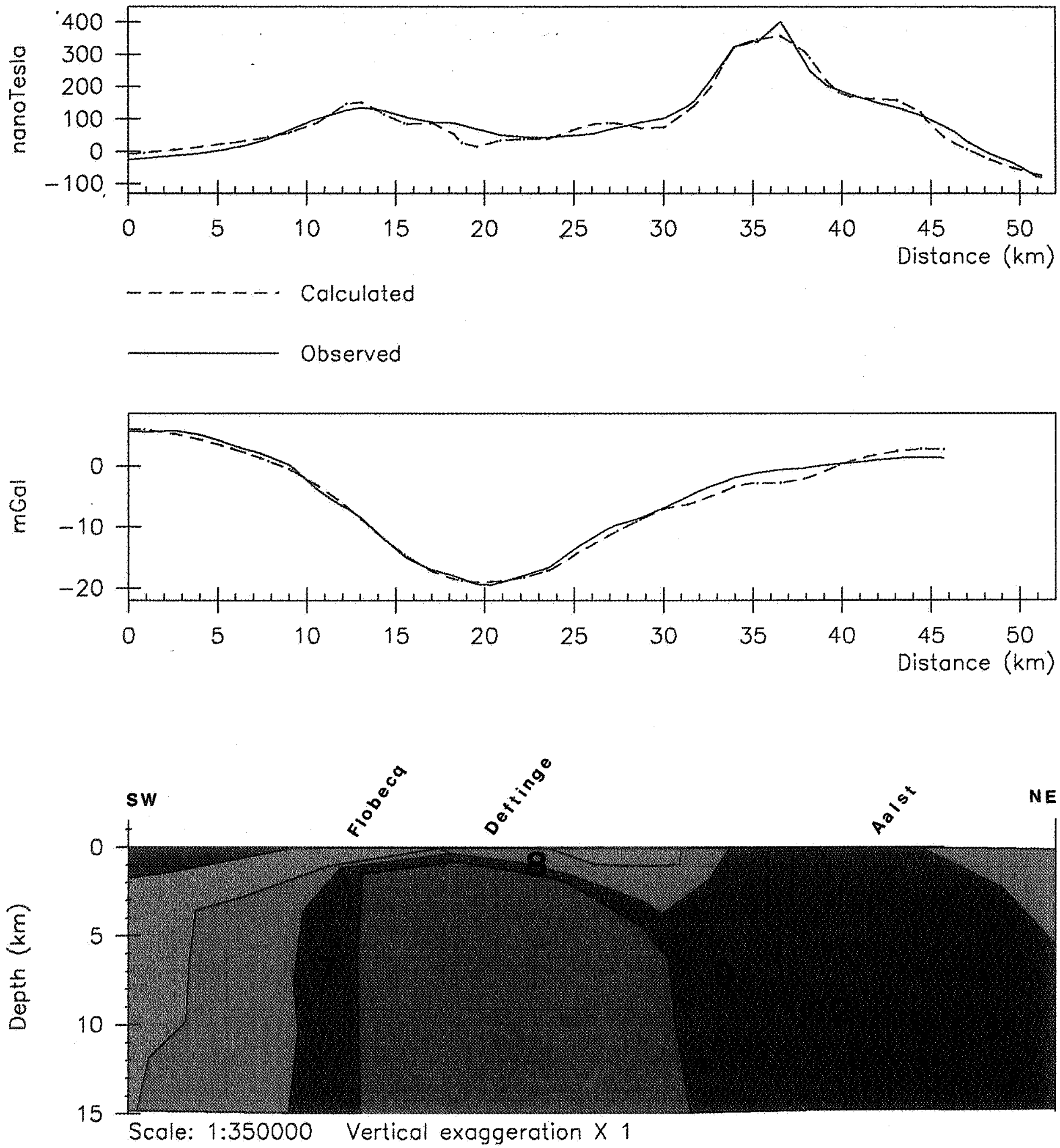

Figure 9. Modelled geological section along profile 3 (location see figure 4), across eastern gravity low. Upper figure: magnetic curve; middle figure: gravity curve; lower figure: geological model. Polygon numbers and their petrophysical properties assumed in the model are presented in table 1. Red: granite. Green: Tubize group. Purple: Oisquercq group. Orange: upper Cambrian to Silurian sediments. Blue: Devonian and Carboniferous sediments.

It is shown in green in profiles 1 to 4. From the modelling, and according to the magnetic curves, it appears that the Tubize group surrounds the granite on all sides. The bulk of it lies to the north of the granite, in the core of the main antiform of the Brabant Massif. Its magnetic susceptibility shows strong variation. Petrophysical measurements gave figures between 0.0005 and 0.02 SI units on hand specimens from shallow drill cores (De Vos *et al.*, 1993c). However, the average magnetic susceptibility at depth, which determines the magnetic field, must be generally higher to account for the observed magnetic field.

A magnetic susceptibility between 0.02 SI and 0.10 SI was used in the models (table 1). In the northern and southern areas, away from the granite, the magnetic susceptibility appears to be lower than above the granite. In the longitudinal direction, the

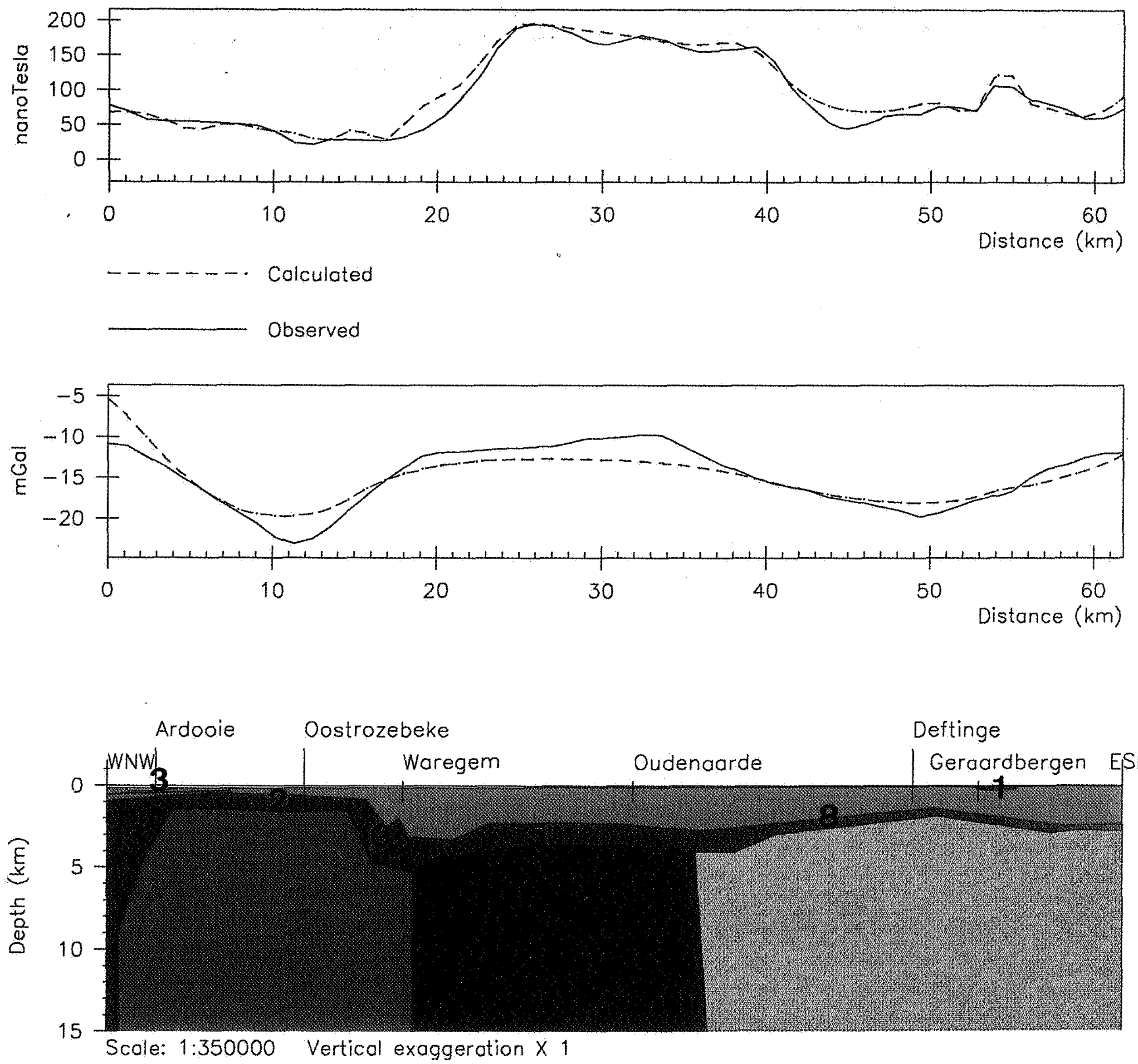

Figure 10. Modelled geological section along profile 4 (location see figure 4), longitudinal section. Upper figure: magnetic curve; middle figure: gravity curve; lower figure: geological model. Polygon numbers and their petrophysical properties assumed in the model are presented in table 1. Red, brown and bluish purple: granite. Green: Tubize group. Purple: Oisquercq group. Black (polygon 1): Geraardsbergen diorite. Light grey (polygon 3): Ardooie porphyry.

magnetism of the Tubize group is not uniform either. It is higher in the area cut by profile 2, both to the south and the north of the granite; a magnetic susceptibility of 0.04 SI matches the observations (polygons 4 and 6). Polygon 4 corresponds to the magnetic anomaly in the center of figure 2. To the west (polygons 1 and 3) and the east (polygons 7 and 9) a lower susceptibility of 0.02 SI was used in the models.

The highest susceptibility is associated with the rocks right above the granite, where a figure of 0.05 SI was used in the west (polygon 2), and 0.10 SI in the center and east (polygons 5 and 8). Profile 4 (fig.10) shows that the central segment of the granite coincides with a positive magnetic anomaly. In the corresponding model, the Tubize group overlying the granite (polygon 5), with a susceptibility of 0.10 SI, must be thicker than elsewhere. Alternatively, the Tubize group could be thinner and more magnetic. In any case, the magnetite content of the rocks right above the granite has to be higher than elsewhere in the Tubize group to explain the observations.

In profile 4, the westernmost part of the Tubize group (polygon 13 in figure 10), west of the granite, shows very low magnetic susceptibility (0.004 SI) similar to the Oisquercq group.

In the northern part, along the main antiform axis of the Brabant Massif, the magnetite bearing rocks do not always have the same density. Generally, a density of 2.72 was used for the Tubize group (table 1), but local deviations are necessary to make the model fit the observations. An antiform core with a higher density is postulated in profile 2 (polygon 11), and a core with a lower density and a slightly higher susceptibility in profile 3 (polygon 12).

These variations in density and magnetic susceptibility are compatible with the layered nature of the Tubize group metasedimentary rocks, which are made up of denser phyllitic rocks and less dense arenitic ones, and a magnetite content varying strongly between beds, and not related to grain size as observed in outcrops (Vander Auwera and André, 1985). The degree of continuity of individual beds is unknown on the scale of the map.

5.4. THE OTHER ROCKS

One small positive magnetic anomaly does not originate from the Tubize group. It appears in the eastern portion of profile 4 (polygon 1) and it can be explained by a shallow intrusive dioritic body at Geraardsbergen, reached in some drill holes. Its susceptibility was determined at 0.034 SI in one sample (De Vos *et al.*, 1993c). This diorite causes a small, weak magnetic anomaly that can be observed in fig. 2 as a green patch near X = 115 and Y = 160 km.
A different intrusive body is represented at Ardooie as polygon 3 in profile 4 (figure 10). It consists of a pale porphyritic rock found in cuttings in several boreholes. Its small density slightly influences the gravity curve (figure 10).

The sedimentary rocks belonging to the Oisquercq group were drawn as separate polygons (purple) in the profiles, with a density of 2.70 g/cm^3 and a weak magnetic susceptibility of 0.004 SI.
The Mousty formation of upper Cambrian age, and the Tremadoc (lower Ordovician) sediments appear in yellow in profile 2, having a density of 2.75 and no magnetism. The younger Ordovician and the Silurian were grouped as one type of polygons (orange), also with a density of 2.75 g/cm^3 and zero magnetic susceptibility. Actually, the modelling of these units is less reliable than the modelling of the granite and the Tubize group, because of the wide range of measured densities in these upper Cambrian to Silurian rock types (De Vos *et al.*, 1993c). The models shown in the profiles are only tentative, and the structures are based on the subcrop map (fig.4).

The Devonian-Carboniferous sediments at the southwestern edge of the profiles were drawn as a thin cover, in accordance with borehole information. Their petrophysical differentiation is undocumented, but their density is low in comparison with the lower Palaeozoic rocks, and from the absence of anomalies on the magnetic total field map we can deduce a very low magnetic susceptibility.

6. STRUCTURAL OUTLINE AND CONCLUSIONS

The modelling was carried out to a depth of about 15 km. It should be kept in mind that the best geophysical constraints exist for the granite and the Tubize group units. Boreholes penetrate the basement only to about 400 m in the investigated area. Filling in geological units other than the granite becomes more and more speculative with greater depth.

Profiles 1, 2 and 3 illustrate the changes from west to east across the Brabant Massif. The polygons drawn in the models do not show faulting explicitly. Nevertheless, the granite is likely to be limited by vertical faults, constituting a horst structure.
The eastern profile (3) shows the synform between the granite and the Tubize group. The infilling sedimentary rocks comprise the Oisquercq group, the Mousty formation (upper Cambrian), the Tremadoc and the middle and upper Ordovician. It is probably a syncline bordered by graben-like faults. This synclinal structure gradually disappears to the west (profiles 2 and 1).
These and other subvertical faults, with a strike parallel to the longitudinal axis of the Brabant Massif, probably account for the sudden geological changes from southwest to northeast across the Massif. The location of these faults corresponds to magnetic lineaments (see fig.2 and also Chacksfield *et al.*, 1993) and gravity lineaments (fig. 6).

It is very likely that the granite was uplifted through geological times because of its buoyancy, causing the horst structure. Still, the lower Cambrian rocks constituting the core of the Brabant antiform, to the north of the granite, appear even more uplifted. This may be the result of the main phase of the Acadian orogeny in this area, which apparently affected northern areas more than southern ones, as witnessed by higher dip angles in the north, and by the pattern of the distribution of metamorphic grade (Geerkens and Laduron, 1995). This orogeny probably dates from the lower Devonian, as inferred from geochronological measurements (Michot *et al.*, 1973, André *et al.*, 1981) and by the angular disconformity between upper Silurian and middle Devonian in the Brabant outcrop area, and was contemporaneous with the Acadian orogeny in eastern North America and the British Isles (McKerrow, 1988).

The granite may have functioned as a stable wall stopping the folding from the north and causing upthrusting of the folded rocks. This interpretation assumes that the antiform in the core of the Brabant Massif is caused by Acadian folding and thrusting towards the south. It would also mean that the intrusion is older than the Acadian orogeny.
The granite is most likely of the same age and genetically related to the volcanic arc above it, a statement already made by de Magnée (1949). The volcanic rocks mainly originated during the lower Ashgill (Van Grootel *et al.*, 1996), and have a calc-alkaline signature, pointing to compression-related subduction (André *et al.*, 1986).
The large batholith at depth is either contemporaneous with the volcanism, emplaced in a syn-orogenic transtensional fault zone, or slightly younger, related to a relaxation of the compression, which would have occurred as a post-orogenic phase during the early Silurian, contemporaneous with strong subsidence (Verniers & Van Grootel, 1991).

It is worth noting that the western part of the granite, in the area of Oostrozebeke, has a large extension in transverse (NE-SW) direction (fig.3), unlike the rest of the granite. This could mean that the intrusion itself followed two pre-existing axes of crustal weakness: the main axis oriented west-north-west, and a transverse axis oriented north-east.
The pre-existing axes determining the shape of the intrusion could be related to the initial rifting of the Rheic ocean in the Arenig, when Eastern Avalonia split off from Gondwana (Trench *et al.*, 1992), causing a normal fault which corresponds to the present-day longitudinal axis of the granite, and a transform fault corresponding to the present-day transverse north-east axis.

As stated above, the southern margin of the granite, based on the second vertical derivative of the gravity field, projected on a map, is not rectilinear (fig.6). It consists of line segments roughly coinciding with a longitudinal fault zone called "bande failleuse antésilurienne" by Legrand (1968), "Oudenaarde-Bierghes fault zone" by André & Deutsch (1985), "Nieuwpoort-Asquempont fault zone" by De Vos *et al.*(1993a) and "zone faillée du Brabant" by Hennebert (1994).
From the present modelling, it appears that this longitudinal fault zone probably originated as a deep strike-slip fault or shear zone running parallel to the southern edge of the granite. This can be interpreted in two different ways: either the subduction was oblique, and the strike-slip fault is of the same age as the granite crystallization during subduction, or it is much younger than the granite (and unrelated to the subduction), and it left the granite unaffected because of its compact and resistant nature. A third possibility is the combination of subduction-related origin with later reactivation.
Fault breccias observed in boreholes near Oudenaarde and Geraardsbergen (fig. 6) are not located in the longitudinal fault zone, as speculated by Legrand (1968) but on transverse faults, to the north of the longitudinal shear and not directly related to it.
However, the mylonites of Bierghes, to the east of our study area, and the incipient foliation at Deerlijk-Harelbeke just south of the granite, dated by André & Deutsch (1985) in the middle Devonian, are situated in the longitudinal fault zone and form a part of the longitudinal strike-slip event. This favours a middle Devonian strike-slip age, which means younger than the granite, without excluding the possibility of two or more strike-slip events along the same shear zone.

It is interesting to note that the longitudinal and transverse faults, along with some other alignments, correspond to two main directions in a working model of a sinistral Riedel shear, used to explain some hydrochemical and structural characteristics in the Brabant Massif basement, acting as possible metallotects (Sterpin *et al.*,1996, in preparation). This does not solve the problem of when this fault pattern first emerged; it rather suggests that the faults were reactivated once they were put into place. Also, dextral and sinistral shear may have occurred along the same fault zone at different times.

The longitudinal fault zone south of the granite would also have acted in later geological times as a zone of vertical movement along which the granite was further uplifted.
The age of the transverse faults and the relative movement taking place along them at different geological times is still a matter of speculation. Block faulting with both a vertical and a strike-slip component probably occurred throughout Variscan and Alpine times. The southern antiform overlying the southeastern part of the granite is probably caused by this Variscan and/or Alpine block faulting in combination with batholith buoyancy.

Some movement, along both longitudinal and transverse faults, still occurs at present, as witnessed by recent seismicity in the Brabant Massif, especially the pattern of destruction caused by the Oudenaarde earthquake of 1938 (Camelbeeck, 1993), which shows a longitudinal axis south of the granite and a transverse axis through Oudenaarde; the depth of its hypocentre was estimated between 15 and 22 km. Unfortunately, the relative displacement during this earthquake could not be reconstructed due to a lack of adequate observations.
According to Ahorner (1970) the present late Alpine stress field in western Europe causes dextral wrench-faults along the southern margin of the Brabant

Massif, which suggests recent dextral movement along the longitudinal fault zone south of the granite.

7. ACKNOWLEDGEMENTS

This study was funded by the Afdeling Natuurlijke Rijkdommen en Energie (ANRE: Division of Natural Resources and Energy) of the Ministerie van de Vlaamse Gemeenschap (Ministry of the Flemish Community), as part of a research program on the Brabant Massif initiated by its director P. Vansteelandt. The recent gravity surveys in the study area, executed by the ORB-KSB, are also part of this programme. The study was partly carried out at the Laboratory of Applied Geology headed by W. De Breuck, University of Gent. Critical comments by T. Pharaoh and J. Verniers are gratefully acknowledged.

8. REFERENCES

AHORNER, L. 1970. Seismo-tectonic relations between the graben zones of the Upper and Lower Rhine Valley. *In*: J.H. Illies and St. Mueller, Graben Problems: Proc. Intl. Rift Symp. 1968. Intl. Upper Mantle Project Scientific Repôrt n° 27. Schweizerbartsche Verlag, Stuttgart, 155-166.

ANDRE, L. 1991. Guidebook to the excursion on the stratigraphy and magmatic rocks of the Brabant Massif, Belgium. 2. Caledonian magmatism. *In:* Proceedings of the international meeting on the Caledonides of the Midlands and the Brabant Massif, Brussels 1989 (Eds André, L., Herbosch, A., Vanguestaine, M. and Verniers, J.). *Annales de la Société Géologique de Belgique:* 114-2, 315-323.

ANDRE, L., DEUTSCH, S. & MICHOT, J. 1981. Données géochronologiques concernant le développement tectono-métamorphique du segment Calédonien brabançon. *Annales de la Société Géologique de Belgique,* 104: 241-253.

ANDRE, L. & DEUTSCH, S. 1985. Very low-grade metamorphic Sr isotopic resettings of magmatic rocks and minerals; evidence for a late Givetian strike-slip division of the Brabant Massif, Belgium. *Journal of the Geological Society, London,* 142: 911-923.

ANDRE, L., HERTOGEN, J. & DEUTSCH, S. 1986. Ordovician-Silurian magmatic provinces in Belgium and the Caledonian orogeny in middle Europe. *Geology,* 14: 879-882.

BARANOV, V. 1953. Calcul du gradient vertical du champ de gravité ou du champ magnétique mesuré à la surface du sol. *Geophys. Prosp,* 1: 171-191.

BELGISCHE GEOLOGISCHE DIENST/SERVICE GEOLOGIQUE DE BELGIQUE, 1964. Aeromagnetische kaart/Carte aéromagnétique, scale 1 : 300 000, printed at Militair Geografisch Instituut, Brussels.

BUSBY, J., KIMBELL, G. & PHARAOH, T. 1993. Integrated geophysical-geological modelling of the Caledonian and Precambrian basement of southern Britain. *Geological Magazine,* 130/5: 593-604.

CAMELBEECK, T. 1993. Mécanisme au foyer des tremblements de terre et contraintes tectoniques: le cas de la zone intraplaque belge. Ph.D. thesis, UCL, Louvain-la-Neuve.

CHACKSFIELD, B., DE VOS, W., D'HOOGE, L., DUSAR, M., LEE, M., POITEVIN, C., ROYLES, C., VERNIERS, J. 1993. A new look at Belgian aeromagnetic and gravity data through image-based display and integrated modelling techniques. *Geological Magazine,* 130/5: 583-591, Cambridge.

DE MAGNEE, I. 1949. Commentaire géologique sur la nouvelle carte gravimétrique de la Belgique. *Bulletin de la Société belge de Géologie,* 57/3: 576-587.

DE MEYER, F. 1983. Gravity interpretation of the western flank of the Brabant Massif. *Koninklijk Meteorologisch Inst. België,* Publicaties serie A/111: 1-34.

DE MEYER, F. 1984. Two structural models for the western flank of the Brabant Massif. *Geophys. Prospect.,* 32: 37-50.

DE VOS, W. 1993. Geologisch onderzoek in het Massief van Brabant. *In:* Studiedag BNRE, Geologische kartering en geologisch onderzoek in het Vlaamse gewest, Brussel, 7 dec.1993.

DE VOS, W., VERNIERS, J., HERBOSCH, A. & VANGUESTAINE, M. 1993a. A new geological map of the Brabant Massif, Belgium. *Geological Magazine,* 130/5: 605-611.

DE VOS, W., CHACKSFIELD, B., D'HOOGE, L., DUSAR, M., LEE, M., POITEVIN, C., ROYLES, C., VANDENBORGH, T., VAN EYCK, J. & VERNIERS, J. 1993b. Image-based display of Belgian digital aeromagnetic and gravity data. *Belgische Geologische Dienst, Professional Paper,* 263.

DE VOS, W., POOT, B., HUS, J. & EL KHAYATI, M. 1993c. Geophysical characterization of lithologies from the Brabant Massif as a contribution to gravimetric and magnetic modelling. *Bulletin de la Société belge de Géologie,* 101/3-4: 173-180.

ELKINS, T.A. 1951. The second derivative method of gravity interpretation. *Geophysics,* XVI/1: 29-50.

EVERAERTS, M. 1993. Geofysische modellering, deelrapport van "Voorbereidend onderzoek naar de aanwezigheid van metallische mineralisaties in de sokkel van Vlaanderen", unpublished report, BNRE and Univ. Gent.

GEERKENS, B. & LADURON, D. 1995. Etude du métamorphisme du Massif du Brabant. Unpublished report, BNRE and Univ. Louvain-la-Neuve.

HENDERSON, R.G. & ZIETZ, I. 1949. The computation of the second vertical derivative of the geomagnetic field. *Geophysics,* XIV: 517.

HENNEBERT, M. 1994. Rôle possible des structures profondes du Massif du Brabant dans l'évolution des bassins sédimentaires post-calédoniens (Belgique et Nord-France). *Annales de la Société Géologique de Belgique,* 116/1: 147-162.

JONES, L. 1949. Le levé gravimétrique de la Belgique 1947-1948. *Bulletin de la Société belge de Géologie*, 57/3: 568-575.

LEE, M.K. 1989. Upper crustal structure of the Lake District from modelling and image processing of potential field data. *British Geological Survey, Technical Report* WK/89/1.

LEGRAND, R. 1968. Le Massif du Brabant. *Service Géologique de Belgique, Mémoire*, 9, 148 pp.

MARSON, I. & KLINGELE, E.E., 1993. Advantage of using the vertical gradient of gravity for 3-D interpretation. *Geophys. Prosp.*, 58: 1588-1595.

McKERROW, W.S. 1988. Wenlock to Givetian deformation in the British Isles and the Canadian Appalachians. *In:* The Caledonian-Appalachian Orogen, Eds Harris, A & Fettes, D. *Geological Society Special Publication*, 38: 437-448.

MICHOT, J., FRANSSEN, L. & LEDENT, D. 1973. Preliminary age measurements on metamorphic formation from the Ardennes anticline and the Brabant Massif (Belgium). *Fortschr. Miner.*, 50: 107-109.

MORELLI, C., 1961. Gravimetria. *Collana di scienze terrestri*, 2, Udine.

NETTLETON, L., 1939. Determination of density for reduction of gravimeter observations. *Geophysics*, 4: 176-183.

PEDLEY, R., 1991. GRAVMAG User Manual: Interactive 2.5D gravity and magnetic modelling program. *British Geological Survey.*

PETERS, L.J., 1949. The direct approach to magnetic interpretation and its practical application. *Geophysics*, XIV: 290.

PHARAOH, T., MOLYNEUX, S., MERRIMAN, R., LEE, M. & VERNIERS, J. 1993. The Caledonides of the Anglo-Brabant Massif reviewed. *Special issue on the Caledonides of the Anglo-Brabant Massif. Geological Magazine*, 130/5: 561-562.

POITEVIN, C., 1987. Levé gravimétrique de la région d'Ardooie. Observatoire Royal de Belgique, Bruxelles. Unpublished report for Belgian Geological Survey.

POITEVIN, C. 1989. Gravity anomalies in the Ardooie area. Abstract. *International Meeting on the Caledonides of the Midlands and the Brabant Massif, Brussels 1989*, 38.

POITEVIN, C., 1992. Levé gravimétrique de la région d'Oudenaarde. Observatoire Royal de Belgique, Bruxelles. Unpublished report for Ministry of Flemish Community.

RASMUSSEN, R. & PEDERSON, L.B., 1979. End correction in potential field modelling. *Geophys. Prosp.* 27: 749-760.

ROSENBACH, O., 1953. A contribution to the computation of the second derivative from gravity data. *Geophysics*, XIV: 290.

SHUEY, R.T. & PASQUALE, A.S., 1973. End correction in magnetic profile interpretation. *Geophysics*, 38: 507-512.

STERPIN, M., DE VOS, W. & DE BREUCK, W., 1996. Hydrochemistry of the Brabant Massif aquifer. *Bulletin de la Société belge de Géologie.* Brussels (in preparation).

TRENCH, A., TORSVIK, T. & McKERROW, W., 1992. The palaeogeographic evolution of Southern Britain during early Palaeozoic times: a reconciliation of palaeomagnetic and biogeographic evidence. *Tectonophysics*, 201: 75-82.

VANDER AUWERA, J. & ANDRE, L., 1985. Sur le milieu de dépôt, l'origine des matériaux et le faciès métamorphique de l'Assise de Tubize (Massif du Brabant, Belgique). *Bulletin de la Société belge de Géologie*, 94/2: 171-184.

VAN GROOTEL, G., VERNIERS, J., GEERKENS, B., LADURON, D., VERHAEREN, M., HERTOGEN, J. & DE VOS, W., 1996. Timing of subduction-related magmatism, foreland basin development, metamorphism and inversion in the Anglo-Brabant fold belt. *Geological Magazine* (submitted).

VERNIERS, J., ANDRE, L., HERBOSCH, A. & VANGUESTAINE, M., 1991. Introduction to the international meeting on the Caledonides of the Midlands and the Brabant Massif. *Proceedings of the international meeting on the Caledonides of the Midlands and the Brabant Massif, Brussels 1989. Annales de la Société Géologique de Belgique,* 114/1.

VERNIERS, J. & DE VOS, W., 1995. Recent research on the Brabant Massif. *Studia geophysica et geodaetica*, 39/3: 347-353, Prague.

VERNIERS, J. & VAN GROOTEL, G., 1991. Review of the Silurian in the Brabant Massif, Belgium. *In:* Proceedings of the international meeting on the Caledonides of the Midlands and the Brabant Massif, Brussels 1989 (Eds André, L., Herbosch, A., Vanguestaine, M. and Verniers, J.). *Annales de la Société Géologique de Belgique,* 114/1: 163-193.

Manuscript received on 12.02.1996 and accepted for publication on 8.04.1996.